

Damping Of Power System Oscillations Using CSC In Coordination With SVS Auxiliary Controller

Dr. Narendra Kumar, P.R. Sharma

Abstract. In this paper an SVS controller, known as the combined reactive power and frequency (CRPF) auxiliary controller has been developed and incorporated in the SVS control system located at the middle of a series compensated long transmission line in coordination with controlled series compensation (CSC) along with Induction machine damping unit (IMDU) coupled to T-G shaft after Intermediate Pressure (IP) turbine to achieve its optimal damping effect for Torsional oscillations. Studies are conducted on a system having a similar spread of the torsional modes as the first IEEE benchmark model. The proposed SVS auxiliary controller in coordination with CSC with its bang – bang form of control is very effective in damping power system oscillations over a wide operating range thus enhancing the Transient performance of the power system.. A digital Time domain simulation study has been performed using a nonlinear system model, to illustrate the effectiveness of the proposed damping controller for power system oscillations under large disturbance conditions.

Keywords: Static Var System, CRPF, Auxiliary controller, Subsynchronous resonance, Controlled series compensation

I. INTRODUCTION

DAMPING of power oscillations associated with the generator rotor swings is an important and challenging task in the power industry. These low frequency oscillations arise due to the dynamics of inter area power transfer and exhibit poor damping at high power transfer levels. Oscillations associated with single generator (Local Modes) have frequencies in the range of 0.8-1.8 Hz. The inter area modes have the frequency of oscillations in the range 0.2-0.5 Hz and involve large group of generators swinging against each other. The stability of these low frequency oscillations is a pre requisite for secure operation of system after critical contingencies.

With the advent of fast acting, power electronic based FACTS controllers like SVS, TCSC, SSSC, STATCOM, TCPAR and UPFC, it is feasible to enhance the damping of power system oscillations effectively at low cost [4,5,7,11]. In recent years SVS has been employed to an increasing extent in modern power systems [1,4,10] due to its capability to work as Var generation and absorption

systems. Besides, voltage control and improvement of transmission capability SVS in coordination with auxiliary controllers [3,4,6,10] can be used for damping of power system oscillations. Damping of power system oscillations plays an important role not only in increasing the transmission capability but also for stabilization of power system conditions after critical faults, particularly in weakly coupled networks.

The controlled series compensation is one of the novel technique under FACTS philosophy for damping of power system oscillations [5]. D. Povh and Mihalic proposed the application of CSC and SVC for transient stability enhancement of an ac transmission system. Noroozian, M et. al. [6] proposed a robust control strategy for thyristor controlled series capacitor and static VAr systems to damp electromechanical oscillations. Larsen et al [2] have presented the design concepts and a systemic approach for the selection of input signals for FACTS damping controllers based on various damping controller design indices. The angular difference of two remote voltages on each side of TCSC is chosen as damping controller input Control strategies for damping of electromechanical power oscillations using an energy function method have been proposed by Gronquist et al in [3] Chaudhuri, B. Pal et al designed a multiple – input Single output (MISO) controller for TCSC to improve damping of critical inter area modes using global stabilizing signals[12]

In the present literature it is seen that the system dynamics has not been properly taken into account as a result the models are less sensitive towards the voltage overshoots due to fast switching of controlled capacitors.

In the present paper the CRPF SVS auxiliary controller along with IMDU has been employed in coordination with controlled series compensation in a long series compensated transmission line A continuous control of mid point located SVS with the bang –bang form of control of CSC is very effective in damping Torsional oscillations. The above coordination provides an efficient and robust control of power oscillations damping for wide range of power transfer under large disturbance conditions.

II. SYSTEM MODEL

The study system consists of a steam turbine driven synchronous generator (a six- mass model) supplying bulk

power to an infinite bus over a long transmission line (IEEE first benchmark model). An SVS of switched capacitor and thyristor controlled reactor type is considered located at the middle of the transmission line which provides continuously controllable reactive power at its terminals in response to bus voltage and combined reactive power and frequency (CRPF) auxiliary control signals. The series compensation is applied at the sending end of the line.

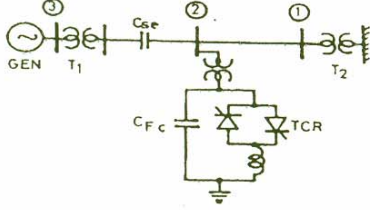


Figure 1. Study System.

A Generator

In the detailed machine model [8] used here, the stator is represented by a dependent current source parallel with the inductance. The generator model includes the field winding 'f' and a damper winding 'h' along d-axis and two damper windings 'g' and 'k' along q-axis. The IEEE type-1 excitation system is used for the generator. In the mechanical model detailed shaft torque dynamics [9] has been considered for the analysis of torsional modes due to SSR. The rotor flux linkages ' ψ ' associated with different windings are defined by:

$$\begin{aligned} \psi_f &= a_1 \psi_f + a_2 \psi_h + b_1 v_f + b_2 i_d \\ \psi_h &= a_3 \psi_f + a_4 \psi_h + b_3 i_d \\ \psi_g &= a_5 \psi_g + a_6 \psi_k + b_5 i_q \\ \psi_k &= a_7 \psi_g + a_8 \psi_k + b_6 i_q \end{aligned} \quad (1)$$

where v_f is the field excitation voltage. Constants a_1 to a_8 and b_1 to b_6 are defined in [9]. i_d , i_q are d, and q axis components of the machine terminal current respectively which are defined with respect to machine reference frame. To have a common axis of representation with the network and SVS, these flux linkages are transformed to the synchronously rotating D-Q frame of reference using the following transformation:

$$\begin{bmatrix} i_d \\ i_q \end{bmatrix} = \begin{bmatrix} \cos \delta & -\sin \delta \\ \sin \delta & \cos \delta \end{bmatrix} \begin{bmatrix} i_D \\ i_Q \end{bmatrix} \quad (2)$$

where i_D , i_Q are the respective machine current components along D and Q axis. δ is the angle by which d-axis leads the D-axis. Currents I_d and I_q which are the components of the dependent current source along d and q axis respectively are expressed as:

$$\begin{aligned} I_d &= c_1 \psi_f + c_2 \psi_h \\ I_q &= c_3 \psi_g + c_4 \psi_k \end{aligned} \quad (3)$$

where constants c_1 - c_4 are defined in [9]. Substituting eqn.(2) in eqn.(1) and linearizing gives the state and output equation of the rotor circuit as:

$$\begin{aligned} X_R &= A_R X_R + B_{R1} U_{R1} + B_{R2} U_{R2} + B_{R3} U_{R3} \\ Y_{R1} &= C_{R1} X_R + D_{R1} U_{R1} \end{aligned} \quad (4)$$

$$Y_{R2} = C_{R2} X_R + D_{R2} U_{R1} + D_{R3} U_{R2} + D_{R4} U_{R3}$$

where

$$X_R = [\Delta \psi_f \Delta \psi_h \Delta \psi_g \Delta \psi_k], U_R = [\Delta \delta \Delta \omega], U_{R2} = \Delta V_f$$

$$U_{R3} = [\Delta i_D \Delta i_Q], Y_{R1} = [\Delta I_D \Delta I_Q], Y_{R2} = [\Delta I_D \Delta I_Q]$$

B Mechanical System

The mechanical system (fig.2) is described by the six spring mass model. The governing equations and the state and output equations are given as follows:

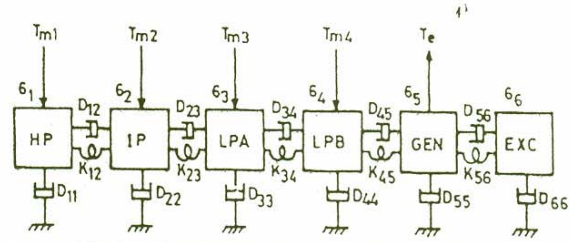


Fig. 2. 6-Spring mass model of mechanical system

$$\delta_i = \omega_i \quad i=1,2,3,4,5,6$$

$$\omega_1 = [-(D_{11} + D_{12})\omega_1 + D_{12}\omega_2 - K_{12}(\delta_1 - \delta_2) + T_{m1}] / M_1$$

$$\omega_2 = [(D_{12}\omega_1 - (D_{12} + D_{22} + D_{23})\omega_2 + D_{23}\omega_3 - K_{12}(\delta_2 - \delta_1) - K_{23}(\delta_2 - \delta_3) + T_{m2}] / M_2$$

$$\omega_3 = [(D_{23}\omega_2 - (D_{23} + D_{33} + D_{34})\omega_3 + D_{34}\omega_4 - K_{23}(\delta_3 - \delta_2) - K_{34}(\delta_3 - \delta_4) + T_{m3}] / M_3$$

$$\omega_4 = [(D_{34}\omega_3 - (D_{34} + D_{44} + D_{45})\omega_4 + D_{45}\omega_5 - K_{34}(\delta_4 - \delta_3) - K_{45}(\delta_4 - \delta_5) + T_{m4}] / M_4$$

$$\omega_5 = [(D_{45}\omega_4 - (D_{45} + D_{55} + D_{56})\omega_5 + D_{56}\omega_6 - K_{45}(\delta_5 - \delta_4) - K_{56}(\delta_5 - \delta_6) + T_e] / M_5$$

$$\omega_6 = [(D_{56}\omega_5 - (D_{56} + D_{66})\omega_6 - K_{56}(\delta_6 - \delta_5) + T_e] / M_6$$

After linearizing the above eqns., the state and output

eqns. can be written as:

$$X_M = A_M X_M + B_{M1} U_{M1} + B_{M2} U_{M2}$$

$$Y_M = C_M X_M \quad (6)$$

Where

$$X_M = [\Delta \delta_1, \Delta \delta_2, \Delta \delta_3, \Delta \delta_4, \Delta \delta_5, \Delta \delta_6, \Delta \omega_1, \Delta \omega_2, \Delta \omega_3, \Delta \omega_4, \Delta \omega_5, \Delta \omega_6]^t$$

$$Y_M = [\Delta \delta_5, \Delta \omega_5]^t, U_{M1} = [\Delta I_D, \Delta I_Q]^t$$

$$U_{M2} = [\Delta i_D, \Delta i_Q]^t$$

C Network

The transmission line (fig.3) is represented by lumped parameter T-circuit. The network has been represented by its α -axis equivalent circuit which is identical with the

itive sequence network. The governing equations of α -axis, T-network representation are derived as follows:

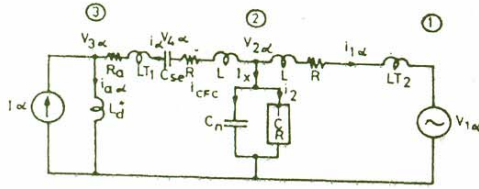


Figure 3. α -axis representation of the network

$$\begin{aligned}
 +L_{T2} di_{1\alpha}/dt &= V_{2\alpha} - V_{1\alpha} - R i_{1\alpha} \\
 +L_A di_{\alpha}/dt &= V_{2\alpha} - (R+R_A) i_{\alpha} - L_d i_{\alpha} - V_{4\alpha} \quad (7) \\
 dV_{2\alpha}/dt &= -i_{2\alpha} - i_{\alpha} - i_{1\alpha} \\
 dV_{4\alpha}/dt &= -i_{\alpha}
 \end{aligned}$$

where $L_A = L_{T1} + L_d$ and $C_n = C + C_{FC}$

Similarly, the equations can be derived for the β -network. The α - β network equations are then transformed to the D-Q frame of reference and subsequently linearised. The state and output equations for the network model are finally obtained as:

$$\begin{aligned}
 \dot{X}_N &= [A_N] X_N + [B_{N1}] U_{N1} + [B_{N2}] U_{N2} + [B_{N3}] U_{N3} \\
 Y_{N1} &= [C_{N1}] X_N + [D_{N1}] U_{N1} + [D_{N2}] U_{N2} + [D_{N3}] U_{N3} \\
 Y_{N2} &= [C_{N2}] X_N, \quad Y_{N3} = [C_{N3}] X_N \quad (8)
 \end{aligned}$$

where,

$$\begin{aligned}
 X_N &= [\Delta i_{1D} \Delta i_{1Q} \Delta V_{2D} \Delta V_{2Q} \Delta i_{1\alpha} \Delta i_{1\beta} \Delta V_{4D} \Delta V_{4Q}]^T \\
 Y_{N1} &= [\Delta i_{2D} \Delta i_{2Q}]^T, \quad Y_{N2} = [\Delta i_{1D} \Delta V_{1Q}]^T, \\
 Y_{N3} &= [\Delta i_{1D} \Delta i_{1Q}]^T \\
 U_{N1} &= [\Delta V_{BD} \Delta V_{BQ}]^T, \quad Y_{N2} = [\Delta i_{1D} \Delta i_{1Q}]^T, \\
 U_{N3} &= [\Delta V_{2D} \Delta V_{2Q}]^T
 \end{aligned}$$

Static Var System

Fig. 4 shows a small signal model of a general SVS. The terminal voltage perturbation ΔV and the SVS incremental current weighted by the factor K_D representing current droop are fed to the reference junction. T_M represents the measurement time constant, which for simplicity is assumed to be equal for both voltage and current measurements. The voltage regulator is assumed to be a proportional-integral (PI) controller. Thyristor control action is represented by an average dead time T_D and a firing delay time T_S . $\Delta\Delta B$ is the variation in TCR susceptance. ΔV_F represents the incremental auxiliary control signal. The α , β axes currents entering TCR from the network are expressed as:

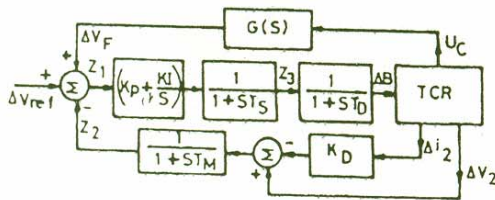


Fig. 4. SVS control system with auxiliary feedback

$$\begin{aligned}
 L_S di_{2\alpha}/dt &= V_{2\alpha} - R_S i_{2\alpha} \\
 L_S di_{2\beta}/dt &= V_{2\beta} - R_S i_{2\beta} \quad (9)
 \end{aligned}$$

where R_S, L_S represent TCR resistance and inductances respectively. The other equations describing the SVS model are:

$$\begin{aligned}
 z_1 &= V_{ref} - z_2 + \Delta V_F \\
 z_2 &= (\Delta V_2 - K_D \Delta i_2) / T_M - z_2 / T_M \\
 z_3 &= (-K_I z_1 + K_P z_2 - z_3 - K_P \Delta V_{ref}) / T_S \quad (10)
 \end{aligned}$$

$$\Delta B = (z_3 - \Delta B) / T_D$$

where $\Delta V_2, \Delta i_2$ are incremental magnitudes of SVS voltage and current, respectively, obtained by linearising

$$V_2 = (V_{2D}^2 + V_{2Q}^2)^{1/2}, \quad i_2 = (i_{2D}^2 + i_{2Q}^2)^{1/2}$$

The state and output eqns. of the SVS model are obtained as:

$$\begin{aligned}
 \dot{X}_S &= [A_S] X_S + [B_{S1}] U_{S1} + [B_{S2}] U_{S2} + [B_{S3}] U_{S3} \quad (11) \\
 Y_S &= [C_S] X_S + [D_S] U_{S1}
 \end{aligned}$$

where

$$\begin{aligned}
 X_S &= [i_{2D} \ i_{2Q} \ z_1 \ z_2 \ z_3 \ \Delta B]^T, \\
 U_{S1} &= [\Delta V_{2D} \ \Delta V_{2Q}]^T, \quad U_{S2} = \Delta V_{ref}, \\
 U_{S3} &= \Delta V_F \\
 Y_S &= [\Delta i_{2D} \ \Delta i_{2Q}]^T
 \end{aligned}$$

III. DEVELOPMENT OF SVS AUXILIARY CONTROLLER

The auxiliary signal U_C is implemented through a first order auxiliary controller transfer function $G(s)$ as shown in fig.5 which is assumed to be:

$$G(s) = \Delta V_F / U_C = K_B (1 + sT_1) / (1 + sT_2)$$

This can be equivalently written as:

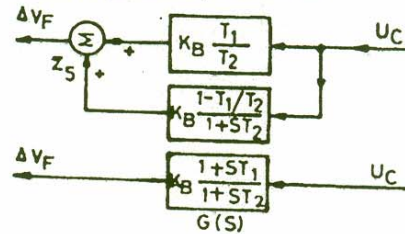


Figure 5. General first-order auxiliary controller

$$G(s) = K_B T_1 / T_2 + K_B (1 - T_1 / T_2) / (1 + sT_2) \quad (12)$$

The state and output equations are given by

$$\begin{aligned}
 \dot{X}_C &= [A_C] X_C + [B_C] U_C \\
 Y_C &= [C_C] X_C + [D_C] U_C \quad (13)
 \end{aligned}$$

where $X_C = [Z_C], Y_C = \Delta V_F, [A_C] = -1/T_2, [B_C] = K_B / T_2 (1 - T_1 / T_2), [C_C] = 1, [D_C] = K_B T_1 / T_2$

A Reactive Power Auxiliary Signal

The auxiliary control signal in this case is the deviation in the line reactive power entering the SVS bus. The reactive power entering the SVS bus can be expressed as:

$$Q_2 = V_{2D} i_Q - V_{2Q} i_D \quad (14)$$

Where i_D, i_Q and V_{2D}, V_{2Q} are the D-Q axis components of the line current i and the SVS bus voltage V_2 respectively. Linearizing eqn. (14) gives the deviation in the reactive power ΔQ_2 which is taken as the auxiliary control signal U_{C1} .

$$U_{C1} = \Delta Q_2 = V_{2D0} \Delta i_Q + i_{Q0} \Delta V_{2D} - V_{2Q0} \Delta i_D - i_{D0} \Delta V_{2Q} \quad (15)$$

B Bus Frequency Auxiliary Signal

The SVS bus frequency is given as:

$$f_{SVS} = d/dt [\tan^{-1}(V_{2Q} / V_{2D})] \quad (16)$$

Linearising eqn. (16) gives the deviation in bus frequency, Δf_{SVS} which is taken as the auxiliary control signal (U_{C2}).

$$U_{C2} = \Delta f_{SVS} = (V_{2D0} / V_{20}^2) \Delta V_{2Q} - (V_{2Q0} / V_{20}^2) \Delta V_{2D} \quad (17)$$

'o' represents operating point or steady state values.

By using eqns 13, 15 & 17, the state and output equation for the CRPF auxiliary controller are obtained as follows:

$$\begin{bmatrix} \dot{X}_{C1} \\ \dot{X}_{C2} \end{bmatrix} = \begin{bmatrix} A_{C1} & 0 \\ 0 & A_{C2} \end{bmatrix} \begin{bmatrix} X_{C1} \\ X_{C2} \end{bmatrix} + \begin{bmatrix} B_{C1} & 0 \\ 0 & B_{C2} \end{bmatrix} \begin{bmatrix} U_{C1} \\ U_{C2} \end{bmatrix}$$

$$[Y_C] = [C_{C1} \ C_{C2}] \begin{bmatrix} X_{C1} \\ X_{C2} \end{bmatrix} + [D_{C1} \ D_{C2}] \begin{bmatrix} U_{C1} \\ U_{C2} \end{bmatrix} \quad (18)$$

Where the state X_{C1} and matrices A_{C1}, B_{C1}, C_{C1} and D_{C1} correspond to reactive power auxiliary controller and the state X_{C2} and matrices A_{C2}, B_{C2}, C_{C2} and D_{C2} correspond to the bus frequency auxiliary controller.

C Induction Machine Damping Unit (IMDU)

The property of induction machine to act as a generator or motor is utilized to absorb the mechanical power when there is excess and to release it when there is a deficiency. Since the machine comes into operation during transients only, it is designed for very high short term rating and very small continuous rating. Consequently the machine has low inertia, low power, small size and low cost. Because of its small mass and tight coupling with the intermediate pressure turbine it has been considered as a single mass unit with IP turbine. Electrically it is connected to the generator bus. The per unit torque (T_{iml}) is given by:

$$T_{iml} = 3s / [(\omega_0 \cdot r_2') \cdot (1 + (s \cdot x_2' / r_2')^2)] \quad (19)$$

and slip $s = (\omega_0 - \omega_1) / \omega_0$

Hence by considering eqn.(17) the mechanical system model is modified as below.

$$M_3 \dot{\omega}_3 = -(D_{23} + D_{33} + D_{34}) \omega_3 + D_{23} \omega_2 + D_{34} \omega_4 + K_{23} \delta_2 - (K_{23} + K_{34}) \delta_3 + K_{34} \delta_4 + T_{m3} + T_{iml}$$

$$T_{iml} = ((3 / (\omega_0 \cdot r_2')) \cdot [1 + (s \cdot x_2' / r_2')^2] - s \cdot \{ (x_2' / r_2')^2 \}) \cdot \Delta s / [(1 + (s \cdot x_2' / r_2')^2)^2] \quad (20)$$

As deviation in slip, $\Delta s = -\Delta \omega_1 / \omega_0$

At normal operating point $\Delta s = 0$,

hence $\Delta T_{iml} = 3 \Delta s / \omega_0 \cdot r_2'$

$$\Delta T_{iml} = -3 \Delta \omega_3 / \omega_0^2 \cdot r_2'$$

$$M_3 \Delta \dot{\omega}_3 = -(D_{23} + D_{33} + D_{34} + 3 / \omega_0^2 \cdot r_2') \Delta \omega_3 + D_{23} \Delta \omega_2 + D_{34} \Delta \omega_4 + (K_{23} + K_{34}) \Delta \delta_3 + K_{34} \Delta \delta_4$$

The damping coefficient term $-(D_{23} + D_{33} + D_{34})$ of intermediate pressure turbine is thus modified to $-(D_{23} + D_{33} + D_{34} + 3 / \omega_0^2 \cdot r_2')$ on application of IMDU, similarly other mechanical equations can be modified to account the damping effect of IMDU for its different locations on the TG shaft.

The state and output equations of the different constituent subsystems along with the auxiliary controller state and output equations are combined to result in the linearised state equations of overall system as:

$$\dot{X}_T = [A] X_T \quad (21)$$

Where,

$$X_T = [X_R \ X_M \ X_E \ X_N \ X_S \ X_C]^T$$

The dimension of the system matrix is, 35.

D. The Controlled Series Compensation (CSC) Scheme

The CSC scheme as shown in fig. (6) has been simulated by step-wise control of the degree of series compensation by means of sections with thyristor by pass switches. The scheme is implemented as follows.

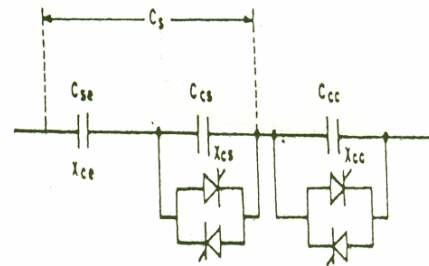
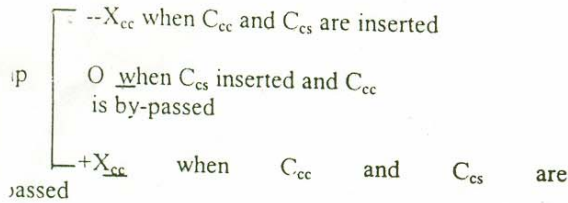


Fig.6 Controlled series compensation scheme

The series capacitor C_s of the line is split into two segments C_{se} and C_{es} with capacitive reactances X_{ce} and X_{es} respectively. C_{se} is left as permanent series compensation while C_{es} is made controllable segment. Another capacitor segment C_{cc} equal in magnitude to that of C_{es} , and having capacitive reactance X_{cc} is also added in series with the line. During steady state condition the capacitor segment remains by passed. The controlled capacitive reactance ' X_{ccap} ' can be defined as:



The control algorithm used senses the angular speed variations from the steady state value and increases or decreases the power transmission by inserting or bypassing the controlled series capacitors when angular speed deviations ($\Delta\omega$) reaches a threshold value of $+\Delta\omega_{Th}$ rad/sec. respectively. Otherwise the controlled series capacitor C_{cc} remain by-passed. In such a way the bang-bang control characteristics of the CSC is achieved. The value of $\Delta\omega_{Th}$ can be adjusted to minimize frequent switching of the controlled series capacitor so the voltage transients are reduced.

IV. A CASE STUDY

The study system consists of 1110 MVA synchronous generator supplying power to an infinite bus over a 400 km. long series compensated single circuit transmission line. The system data and torsional spring mass system data are given in Appendix. The SVS rating of the line has been chosen to be 100 MVAR inductive to 100 MVAR capacitive. 40% series compensation is used at the sending end of the transmission line.

Time Domain Simulations

A digital computer simulation study, using a nonlinear system model, has been carried out to demonstrate the effectiveness of the CRPF auxiliary controller in coordination with CSC under large disturbance conditions for damping power oscillations. Applying a pulsed torque of 20% for 0.1s simulates a disturbance. The simulation study has been carried out at $P=800$ MW. All the self and mutual damping constants are assumed to be zero. Fig. 7.1 and 7.2 show the response curves of the terminal voltage, SVS bus voltage, SVS susceptance, power angle, variation in torsional torques without and with the CRPF auxiliary controller along with IMDU in coordination with CSC after the disturbance respectively. It can be seen that there is a tendency towards instability when no auxiliary controller is used in the SVS control system. The torsional oscillations are stabilized and the coordinated application of CRPF auxiliary controller and CSC damps out voltage power angle and Torsional oscillations effectively and settling time is considerably reduced.

The bang-bang control characteristics of the CSC gives rise to voltage transients. The voltage transients are controlled by closely restricting the reactive power limits of the SVS (0 to 0.4 pu in the present case) and avoiding the frequent switching of controlled capacitor.

V. CONCLUSION

In this paper the effectiveness of coordinated application of CSC and CRPF auxiliary controller along with IMDU has been evaluated for damping power oscillations for a series compensated power system over a wide operating range of power transfer. The following conclusions can be drawn from the time domain simulation study performed.

1. CSC in coordination with CRPF auxiliary controller developed for SVS rapidly damps out the voltage, power angle and Torsional oscillations.

2. CSC generates the voltage transients with its bang-bang form of control. These voltage transients can be controlled by restricting the reactive power limits of SVS and its frequent switching. Thus the proposed damping controller provides an efficient and robust control of power oscillations damping over a wide operating range and under large disturbance conditions.

VI. ACKNOWLEDGEMENT

The work presented in this paper has been performed under the AICTE R&D Project, "Enhancing the power system performance using FACTS devices".

VII. REFERENCES

- Balda J.C. Eitelberg E. and Harley R.G., "Optimal output Feedback Design of Shunt Reactor Controller for Damping Torsional Oscillations", Electric Power System research Vol.10 1986, pp 25-33.
- Einar V. Larsen, Juan J. Sanchez-Gasca and Joe H. Chow, "Concepts for design of FACTS controllers to damp power swings," IEEE Trans. On Power Systems, Vol 10, No.2pp 948-956, May 1995.
- James F. Gronquist, William A. Fernando L. Alvarado and Robert H. Lasseter, "Power oscillation damping control strategies for FACTS devices using locally measurable quantities," IEEE Trans. On Power Systems, Vol 10, No 3, pp 1598-1605, August 1995.
- Narendra Kumar, M.P. Dave, "Application of auxiliary controlled static var system for damping sub synchronous resonance in power systems. Electric Power System Research 37 (1996) 189 - 201.
- X Chen, N. Pahalawaththa, U. Annakkage, C. Kumble, "Controlled series compensation for improving stability of multimachine power systems, IEE Proc.142 (Pt.C) (1995) 361-366
- Noroozian, M. Ghandhari, M. Andersson, G. Gronquist J. Hiskens, "A robust control strategy for shunt and series reactive compensators to damp electromechanical oscillations" IEEE Trans. On Power Delivery, Vol.16, Oct.(2001) 812-817.
- G. N. Pillai, Arindam Gosh, A. Joshi, "Torsional Oscillation Studies in an SSSC Compensated Power System", Electric Power System research 55(2000)57-64.
- Ning, Yang, Q. Liu, J. D. McCalley, "TCSC controller Design for Damping Inter Area Oscillations", IEEE Trans. On Power System, 3(4) (1998) 1304-1310.
- R.S. Ramshaw, K.R. Padiyar, "Generalized system Model for Slip Ring Machines", IEEE Proc.120 (6) 1973.
- K. R. Padiyar, R.K. Varma, "Damping Torque Analysis of Static Var Controllers", IEEE Trans. on Power Systems, 6(2) (1991) 458-465.
- Januszewski, M. Machowski, J Bialek J.W., "Application of direct Lyapunov method to improve damping of power swings by control of UPFC, IEE Proc. Gen. Trans. Distrib. Vol 151, (2004) 252-260

12. Chaudhuri, B. Pal, B.C. "Robust damping of multiple swing modes employing global stabilizing signals with TCSC", IEEE Trans. On Power Syst., Vol.19, pp499-506, Feb.2004

VIII. APPENDIX

Generator data: 1110MVA, 22kV, $R_a=0.0036$, $X_L=0.21$
 $T_{do}=6.66$, $T_{qo}=0.44$, $T_{do}''=0.032$, $T_{qo}''=0.057s$
 $X_d=1.933$, $X_q=1.743$, $X_d''=0.467$, $X_q''=1.144$, $X_d'''=0.312$, $X_q'''=0.312$ put.

IEEE type 1 excitation system:
 $T_R=0$, $T_A=0.02$, $T_E=1.0$, $T_F=1.0s$, $K_A=400$, $K_E=1.0$; $K_F=0.06$ put.
 $V_{Fmax}=3.9$, $F_{in}=0$, $I_{Rmax}=7.3$, $V_R min=-7.3$

Transformer data:
 $R_T=0$, $X_T=0.15$ put. (generator base)

Transmission line data:
 Voltage 400kV, Length 600km, Resistance $R=0.034\Omega / km$, Reactance $X=0.325 \Omega / km$
 Susceptance $B_c=3.7\mu$ mho / km

SVS data:

Six-pulse operation:
 $T_M=2.4$, $T_S=5$, $T_D=1.667ms$, $K_I=1200$, $K_P=0.5$, $K_D=0.01$

Torsional spring-mass system data

Mass	shaft	Inertia H (s)	Spring constant K (p.u. torque/rad.)
HP	HP-IP	0.1033586	25.772
IP	IP-LPA	0.1731106	46.635
LPA	LPA-LPB	0.9553691	69.478
LPB	LPB-GEN	0.9837909	94.605
GEN	GEN-EXC	0.9663006	3.768
EXC		0.0380697	

All self and mutual damping constants are assumed to zero.

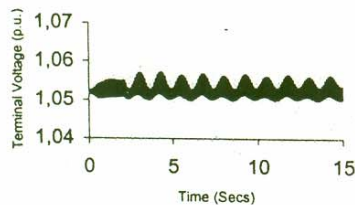


Fig. 7.1 a

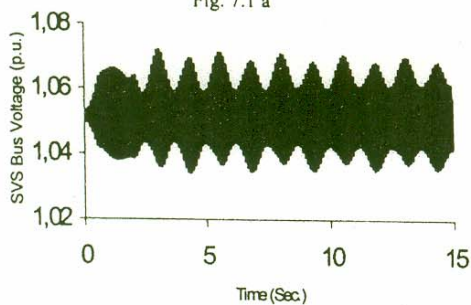


Fig. 7.1 b

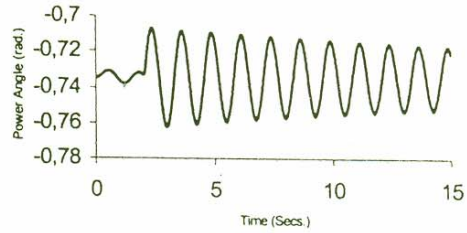


Fig. 7.1 c

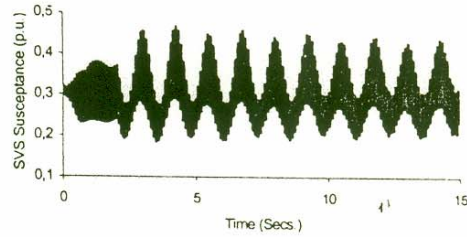


Fig. 7.1 d

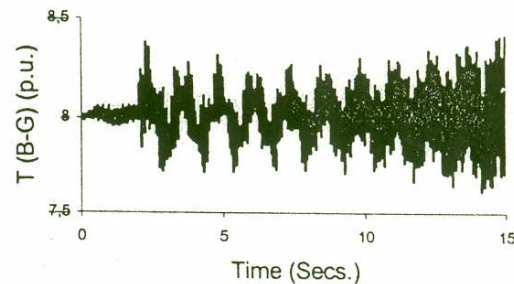


Fig. 7.1 e

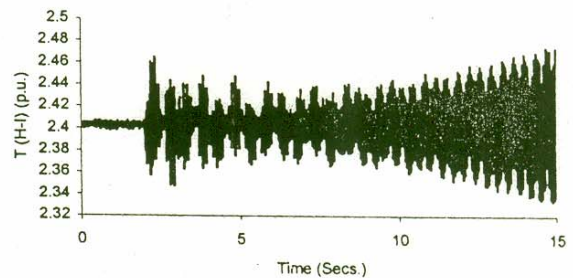


Fig. 7.1 f

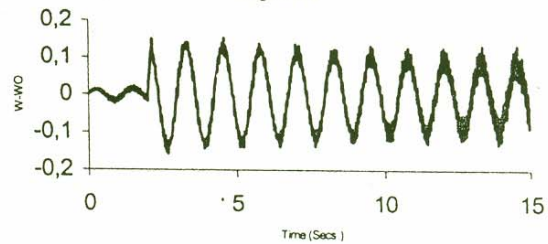


Fig. 7.1 gear

Fig.7.1(a-g) Response curves without any auxiliary controller at $P_g = 800$ MW due to 20% increase in T_{mech} for 0.1 secs (T-circuit Model)

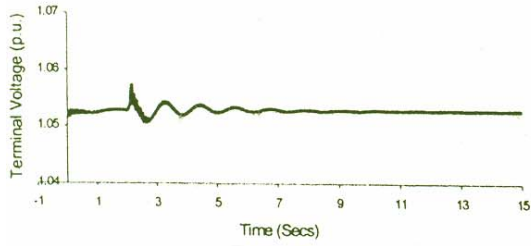


Fig. 7.2 a

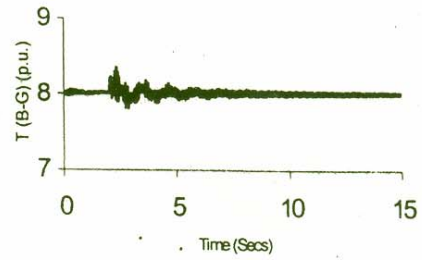


Fig. 7.2 f

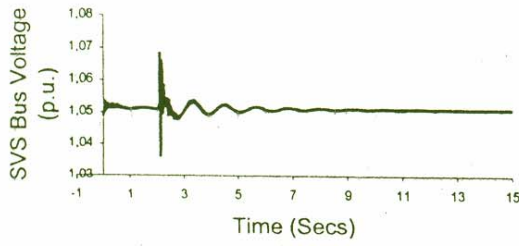


Fig. 7.2 b

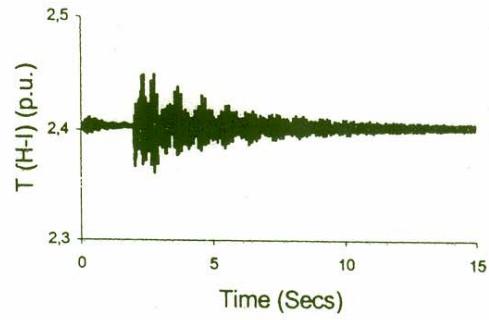


Fig. 7.2 g

S

Fig. 7.2 h

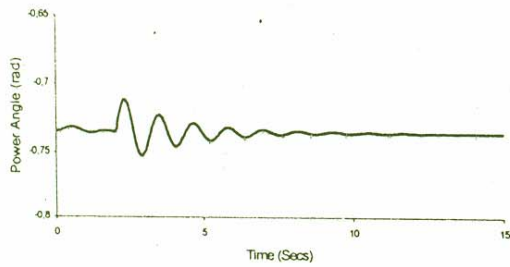


Fig. 7.2 c

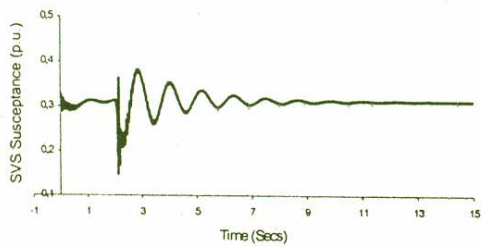


Fig. 7.2 d

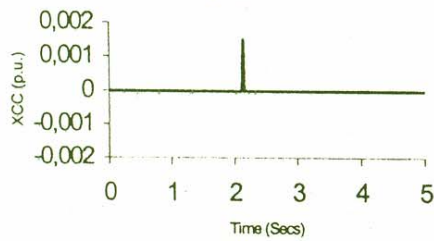


Fig. 7.2 e

Fig. 7.2 (a-h) Response curves with CRPF auxiliary controller and controlled series compensation along with IMDU at $P_g = 800$ MW due to 20% increase in T_{mech} for 0.1 secs (T-circuit Model)